

# How are seasonal prediction skills related to models' performance on mean state and annual cycle?

June-Yi Lee · Bin Wang · I.-S. Kang · J. Shukla · A. Kumar ·  
J.-S. Kug · J. K. E. Schemm · J.-J. Luo · T. Yamagata · X. Fu ·  
O. Alves · B. Stern · T. Rosati · C.-K. Park

Received: 24 March 2008 / Accepted: 19 May 2010 / Published online: 3 June 2010  
© Springer-Verlag 2010

**Abstract** Given observed initial conditions, how well do coupled atmosphere–ocean models predict precipitation climatology with 1-month lead forecast? And how do the models' biases in climatology in turn affect prediction of seasonal anomalies? We address these questions based on analysis of 1-month lead retrospective predictions for 21 years of 1981–2001 made by 13 state-of-the-art coupled climate models and their multi-model ensemble (MME). The evaluation of the precipitation climatology is based on a

newly designed metrics that consists of the annual mean, the solstitial mode and equinoctial asymmetric mode of the annual cycle, and the rainy season characteristics. We find that the 1-month lead seasonal prediction made by the 13-model ensemble has skills that are much higher than those in individual model ensemble predictions and approached to those in the ERA-40 and NCEP-2 reanalysis in terms of both the precipitation climatology and seasonal anomalies. We also demonstrate that the skill for individual coupled models in predicting seasonal precipitation anomalies is positively correlated with its performances on prediction of the annual mean and annual cycle of precipitation. In addition, the seasonal prediction skill for the tropical SST anomalies, which are the major predictability source of monsoon precipitation in the current coupled models, is closely link to the models' ability in simulating the SST mean state. Correction of the inherent bias in the mean state is critical for improving the long-lead seasonal prediction. Most individual coupled models reproduce realistically the long-term annual mean precipitation and the first annual cycle (solstitial mode), but they have difficulty in capturing the second annual (equinoctial asymmetric) mode faithfully, especially over the Indian Ocean (IO) and Western North Pacific (WNP) where the seasonal cycle in SST has significant biases. The coupled models replicate the monsoon rain domains very well except in the East Asian subtropical monsoon and the tropical WNP summer monsoon regions. The models also capture the gross features of the seasonal march of the rainy season including onset and withdraw of the Asian–Australian monsoon system over four major sub-domains, but striking deficiencies in the coupled model predictions are observed over the South China Sea and WNP region, where considerable biases exist in both the amplitude and phase of the annual cycle and the summer precipitation amount and its interannual variability are underestimated.

---

J.-Y. Lee (✉) · B. Wang · X. Fu  
International Pacific Research Center, University of Hawaii,  
POST Bldg, Room 403B, 1680 East-West Road,  
Honolulu, HI 96822, USA  
e-mail: jyilee@soest.hawaii.edu

I.-S. Kang  
School of Earth and Environmental Sciences,  
Seoul National University, Seoul, Korea

J. Shukla  
George Mason University, Arlington, VA, USA

A. Kumar · J. K. E. Schemm  
NCEP/NOAA Climate Prediction Center, Washington, DC, USA

J.-S. Kug  
Korea Ocean Research and Development Institute, Ansan, Korea

J.-J. Luo · T. Yamagata  
FRCGC/JAMSTEC, Yokohama, Japan

O. Alves  
Bureau of Meteorology Research Center, Melbourne, Australia

B. Stern · T. Rosati  
NOAA/GFDL, Princeton University, Princeton, USA

C.-K. Park  
Korean Meteorological Administration, Seoul, Korea

**Keywords** Coupled atmosphere–ocean model · Multi-model ensemble · Precipitation · Mean states · 1-Month lead seasonal prediction · Annual mean · Annual cycle · Monsoon rain domain · Asian–Australian monsoon · ENSO

## 1 Introduction

In dynamical seasonal prediction, errors in the predicted climatology are regarded as systematic biases, which can be removed or “corrected” for improved predictions. However, knowledge of the properties of these biases is necessary for understanding of model’s capabilities and deficiencies in predicting seasonal anomalies. The fidelity of models’ simulation of the climatology may have a close link to its ability in simulation of interannual variability (Fennessy et al. 1994). Sperber and Palmer (1996) showed that models with a more realistic mean state tend to better represent the interannual variability of all Indian monsoon rainfall related to El Niño and Southern Oscillation (ENSO) when the observed SST was given. Sperber et al. (2001) showed that subseasonal empirical orthogonal function (EOF) modes of precipitation and low-level flows in seven AGCMs have errors in the magnitude and location, and which are related to errors in the mean state and could compromise dynamical seasonal predictability. Over Southeast Asia and the tropical Western North Pacific (WNP) regions, realistic simulations of the precipitation anomalies (Fig. 11a in Wang et al. 2004) were achieved by those models that better simulated the climatological precipitation (Fig. 3b in Kang et al. 2002). In addition to climatological means, Gadgil and Sajani (1998) found that the models with realistic simulation of seasonal migration of the rain belt over the Asia–Western Pacific region replicate more realistically the interannual variations of the Indian summer rainfall.

Recent studies have shown that the improvements in a coupled models’ mean climatology generally lead to a more realistic simulation of ENSO–monsoon teleconnection (Lau and Nath 2000; Annamalai and Liu 2005; Turner et al. 2005; Annamalai et al. 2007). Turner et al. (2005) demonstrated that correction of model systematic error in coupled model using ocean-surface heat flux adjustment has significant benefits to towards improving monsoon–ENSO teleconnection, particularly the lag-lead relationship.

Majority of the afore-mentioned studies have used stand-alone atmospheric models forced by observed SST. Treating atmosphere as a slave may limit the level of skill for Atmospheric Model Intercomparison Project (AMIP) type monsoon simulation (Kitoh and Arakawa 1999; Wang

et al. 2004; Wu and Kirtman 2005) and two-tier summer monsoon seasonal prediction (Wang et al. 2005a; Kumar et al. 2005, Nanjundiah et al. 2005; Kug et al. 2008), because the Asian–Australian monsoon is essentially a coupled atmosphere–ocean system (Webster et al. 1998; Meehl et al. 2003; Webster 2006). Here we evaluate the performance of thirteen coupled models that are part of Development of European Multimodel Ensemble system for seasonal-to-interannual prediction (DEMETER) (Palmer et al. 2004) and Asia–Pacific economic cooperation climate center (APCC)/climate prediction and its application to society (CliPAS) projects (Wang et al. 2009). Our assessment will focus on precipitation because the latent heat released in precipitation is a principal atmospheric heat source that drives tropical circulation and because it has profound impacts on agricultural planning and water resource management.

The objective of this study is to identify the strengths and weaknesses of the state-of-the-art coupled climate prediction models in their prediction of precipitation climatology and the impact of the model biases in the mean states on its performance in 1-month lead seasonal prediction of precipitation. Specific questions to be addressed are: (1) how well do the current models forecast the annual mean and the annual cycle (AC) of precipitation? (2) What is the impact of initial condition and forecast lead time on simulating mean states and AC? (3) How are the skills in forecasting the mean state and AC related to the model skills in seasonal prediction?

Section 2 describes the main features of the climate prediction models and the experimental designs for retrospective forecast. In Sect. 3, the annual modes of precipitation in the coupled seasonal predictions are validated against observation. The effect of forecast lead time and initial condition on predicting annual modes is also addressed. In Sect. 4, the assessments are extended to the global monsoon domain and to the important sub-monsoon domains of the Asian–Australian monsoon system using pentad-mean precipitation data. Section 5 explains the relationship between mean state simulation and seasonal prediction. The last section summarizes major points.

## 2 Hindcast experiment data

### 2.1 APCC/CliPAS and DEMETER data

Under the auspices of APCC, the CliPAS project has compiled 14 climate models’ retrospective forecast data for the period 1981–2004. These models consist of seven coupled models and seven stand-alone atmospheric models forced by predicted SST (Wang et al. 2009). The European Union DEMETER project provided seven coupled models’

hindcast data for the period 1980–2001. Refer to Table 1 for full names of acronyms.

Thirteen coupled models are used for the present study from APCC/CliPAS and DEMETER models. A brief summary of these models is presented in Table 2. The models show a large range of model resolution and the number of ensemble member (from 6 to 15). All selected coupled models do not apply any flux correction and they have retrospective hindcasts for the common period of 1981–2001 with four initial conditions starting from February 1, May 1, August 1, and November 1, which yield 1-month lead seasonal forecasts for four seasons, respectively, i.e. March–April–May (MAM), June–July–August (JJA), September–October–November (SON), and December–January–February (DJF).

In the present study, we reconstructed predicted monthly climatology using different forecast lead month based on the 1-month lead seasonal prediction for four initial conditions. Suppose the forecast was initialized on May 1, predictions from June (1-month) to August (3-month lead time) are used for reconstructing AC. The different setting of initial condition for each month may compromise our results. Thus, we investigate the effect of initial condition using NCEP CFS data introduced in the next subsection.

The multi-model ensemble (MME) mean with equal weight has been constructed by interpolating each model's ensemble prediction to a common  $2.5^\circ \text{ lat} \times 2.5^\circ \text{ lon}$  grid comparable to the resolution of the observed data.

## 2.2 The CFS data

NCEP CFS data provide a set of fully coupled retrospective forecasts, which covers a 24-year period of 1981–2004 and consists of 15 ensemble members. The ensemble hindcasts start from each calendar month and extend out 9 months into the future (Saha et al. 2006). Therefore, the dataset allows for a comprehensive assessment of the performance against forecast lead time. In this particular case, the AC is reconstructed using climatological monthly precipitation with the same lead time from 0 to 8 month. The zero-month lead forecast was initialized on the 9, 10, 11, 12, 13, 19, 20, 21, 22, and 23 of the month prior to the target month, the second-to-last day of the previous month, and the first-to-third days of the targeting month.

To identify systematic biases of the model, CFS free coupled runs were also used. There are four coupled CFS runs, each spans a 32-year period from a different initial state (Wang et al. 2005b) and we utilize the last 30-year

**Table 1** Acronym names of institutions and models used in the text

Acronym	Full names
APCC	Asia–Pacific economic cooperation climate center
BMRC	Bureau of meteorology research center (BMRC)
CERFACS	European centre for research and advanced training in scientific computation in France
CES	Climate environment system research center
CFS	Climate forecast system
CliPAS	Climate prediction and its application to society
COLA	Center for ocean–land–atmosphere studies
DEMETER	Development of European multimodel ensemble system for seasonal-to-interannual prediction
ECMWF	European centre for medium-range weather forecasts
FRCGC	Frontier research center for global change
GFDL	Geophysical fluid dynamic lab
GFS	Global forecast system
INGV	Istituto Nazionale de Geofisica e Vulcanologia in Italy
LODYC	Laboratoire d'oc anographie Dynamique et de Climatologie in France
Met Office	The met office in UK
Meteor-France	Centre National de Recherches Meteorologiques in France
MPI	Max-Planck Institute for Meteorologie in Germany
NASA	National aeronautics and space administration
NCEP	National center for environmental prediction
POAMA	Predictive ocean atmosphere model for Australia
SINTEX-F	Scale interaction experiment-FRCGC
SNU	Seoul National University
UH	University of Hawaii

**Table 2** Description of 13 coupled atmosphere–ocean models

Institute (Model index)	Model name	AGCM	OGCM	Ensemble member	Reference
NCEP (M1)	CFS	GFS T62 L64	MOM3 1/3° lat × 5/8° lon L27	15	Saha et al. (2006)
FRCGC (M2)	SINTEX-F	ECHAM4 T106L19	OPA 8.2 2° cos (lat) × 2° lon L31	9	Luo et al. (2005)
SNU (M3)	SNU	SNU T42L21	MOM2.2 1/3° lat × 1° lon L40	6	Kug et al. (2008)
UH (M4)	UH	ECHAM4 T31L19	UH Ocean 1° lat × 2° lon L2	10	Fu and Wang (2004)
GFDL (M5)	CM2.1	AM2.1 2°lat × 2.5°lon L24	MOM4 1/3° lat × 1° lon L50	10	Delworth et al. (2006)
BMRC (M6)	POAMA1.5	BAM 3.0d T47 L17	ACOM3 0.5° lat–1.5° lat × 2.0° lon L31	10	Zhong et al. (2005)
CERFACE (M7)	CERFACE	ARPEGE T63 L31	OPA 8.2 2.0° × 2.0° L31	9	Deque (2001), Delecluse and Madec (1999)
ECMWF (M8)	ECMWF	IFS T95 L40	HOPE-E 1.4° × 0.3°–1.4° L29	9	Gregory et al. (2000), Wolff et al. (1997)
INGV (M9)	INGV	ECHAM4 T42 L19	OPA 8.2 2.0° lat × 2.0° lon L31	9	Roeckner et al. (1996), Madec et al. (1998)
LODYC (M10)	LODYC	IFS T95 L40	OPA 8.0 182GP × 152GP L31	9	Gregory et al. (2000), Delecluse and Madec (1999)
MPI (M11)	MPI	ECHAM5 T42 L19	MPI-OM1 2.5° lat × 0.5°–2.5° lon L23	9	Roeckner et al. (1996), Marsland et al. (2003)
Meteo-France (M12)	Meteo-France	ARPEGE T63 L31	OPA 8.0 182GP × 152GP L31	9	Deque (2001), Madec et al. (1997)
UKMO (M13)	UKMO	HadAM3 2.5 × 3.75L19	GloSea OGCM 1.25° × 0.3–1.25° L40	9	Roeckner et al. (1996), Marsland et al. (2003)

Model index used in figures is also shown

data from each run. Hereafter, we will refer to the free coupled run as the coupled model intercomparison project (CMIP) run.

### 2.3 Observation

The data used for validating retrospective forecast include (1) the climate prediction center merged analysis of precipitation (CMAP) data, which are produced by merging rain gauge data, five kinds of satellite estimates, and precipitation based on the NCEP/NCAR reanalysis (Xie and Arkin 1997), (2) the SST data derived from the improved extended reconstructed sea surface temperature (SST) version 2 (ERSST V2) data (Smith and Reynolds 2004), (3) the precipitation and atmospheric variables from the NCEP-Department of Energy (DOE) reanalysis 2 (NCEP-R2) data (Kanamitsu et al. 2002), and (4) the precipitation data from ECMWF 40-year Reanalysis (ERA-40) data (Uppala et al. 2005).

## 3 Evaluation on the precipitation climatology

In order to better understand the physical processes by which the tropical hydrological cycle and the coupled atmosphere–land–ocean system respond to the solar radiative forcing, Wang and Ding (2008) proposed a simple metrics for assessing climate model performance on

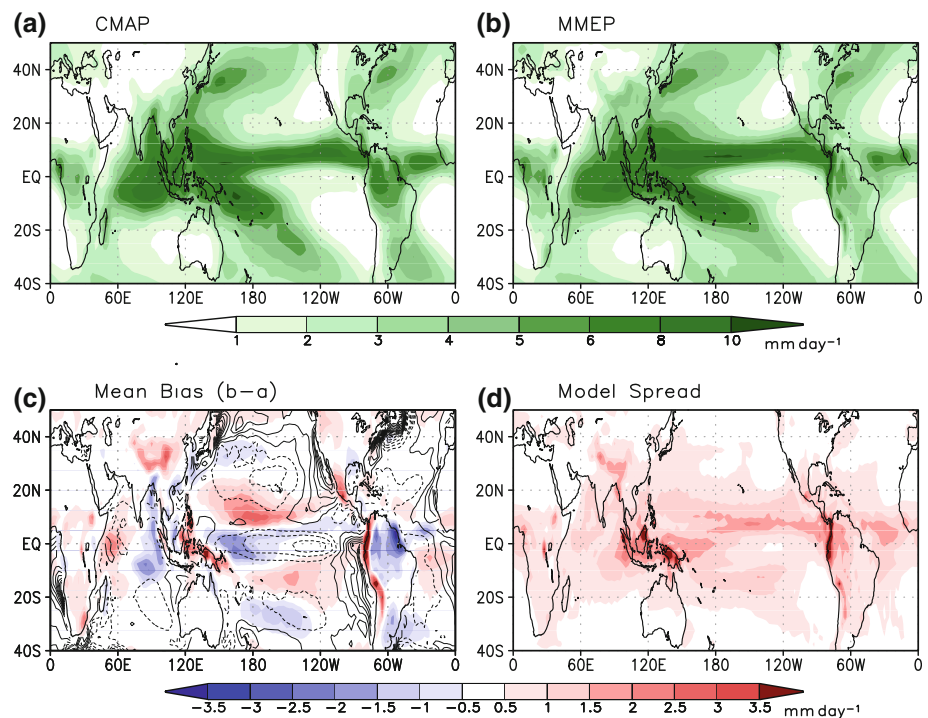
precipitation climatology. The metrics includes (1) the annual mean, (2) the two leading modes of annual variations, i.e. the solstice monsoon mode and the equinox asymmetric mode. In this section, we assess the performance of the 13 coupled models' MME predictions on the annual mean and seasonal mean, the two leading modes of the AC in precipitation in an attempt to identify the common biases in the coupled models for future improvement.

### 3.1 Annual and seasonal mean precipitation

Figure 1 shows climatological long-term annual mean precipitation in observation and 1-month lead seasonal MME prediction. Overall, the MME prediction reproduces the observed features realistically, which includes (1) the major oceanic convergence zones over the tropics: the intertropical convergence zone (ITCZ), the South Pacific convergence zone (SPCZ), and the equatorial-South Indian Ocean (IO) convergence zone, (2) the major precipitation zones in the extra-tropical Pacific and Atlantic, which are associated with the oceanic storm tracks, and (3) remarkable longitudinal and latitudinal asymmetries, which have been discussed in many previous studies (e.g. Annamalai et al. 1999; Goswami et al. 2006; Chang et al. 2005; Wang and Ding 2008).

The common biases in simulating annual mean precipitation are shown in Fig. 1c. The coupled models tend to underestimate precipitation over the eastern IO (including

**Fig. 1** The spatial pattern of long-term mean precipitation derived from **a** observation (CMAP), and **b** 13 coupled models' 1-month lead seasonal multi-model ensemble (MME) prediction. **c** The mean bias defined by the difference **(b)** minus **(a)**. The contours indicate the mean bias of predicted annual mean of sea surface temperature with interval of  $0.3^{\circ}\text{C}$ . **d** Model spread against MME mean defined by the root mean square difference between MME and individual model ensemble predictions



the Bay of Bengal), the equatorial western Pacific, and tropical Brazil, but overestimate precipitation over the Maritime Continent and Philippines where the asymmetric wind–terrain interaction determines rainfall distribution (Chang et al. 2005). The excessive rainfall is also seen along the Andes, Sierra Madrea, and the southern and eastern flanks of the Tibetan Plateau where the wind–terrain interaction influences annual rainfall. Terrain-related precipitation appears more difficult to be correctly replicated by the current coupled models because of their coarse resolution and imperfect parameterization. Precipitation is also overestimated over the central subtropical Pacific in both hemispheres associated with the deficient precipitation over the equatorial western and central Pacific. The biases reflect a slightly northward and westward shift of ITCZ in the models.

In addition to precipitation, SST bias is also shown in Fig. 1c (contours). There exists a significant cold bias in the equatorial Pacific and a large warm bias along and near the eastern boundaries, which may be in part induced by the models poor representation of the stratiform clouds that are observed in many CGCMs (Mechoso et al. 1995).

The uncertainties in the MME prediction are calculated as the standard deviation of individual Model Ensemble (ME)'s departure from the MME mean. Figure 1d shows that the model spread tends to be large over the region where the mean biases are found, especially over the Maritime Continent and oceanic convergence zones. Over Papua New Guinea, Borneo, and the southern Philippines, the model spread is more than 60% of the total annual

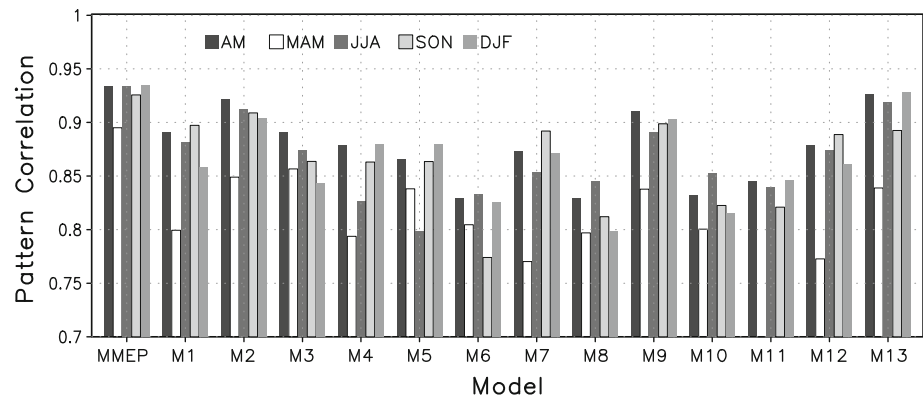
mean value. In addition, a large spread is found along the high elevated terrains (e.g. the equatorial section of Andes), indicating that the model resolution is still one of the major error sources in predicting continental precipitation.

The climatological seasonal means predicted by the coupled models and their MME are also evaluated. In general, the MME and individual MEs realistically predict the seasonal migration of the major rain-bearing regions including the maximum rainfall, its location, and its latitudinal and longitudinal extent. However, large systematic biases are found over the monsoon regions and oceanic tropical convergence zones (not shown).

Figure 2 shows the pattern correlation coefficient (PCC) skill of the individual ME mean and their MME predictions for annual mean and four seasons over the global tropics and subtropics ( $30^{\circ}\text{S}$ – $30^{\circ}\text{N}$ ). It turns out that the JJA and DJF seasons are best predicted while the MAM is least predictable on climatological seasonal precipitation over globe. The seasonal dependency of the skill is particularly larger over the Asian–Australian Monsoon (A–AM) region ( $40^{\circ}\text{E}$ – $160^{\circ}\text{E}$ ,  $30^{\circ}\text{S}$ – $30^{\circ}\text{N}$ ). Over that region, DJF is better predicted than JJA, while the majority of the models have the lowest skill in MAM (not shown). It is noted that some coupled models that share the same atmospheric model but have a different ocean component, such as M8 and M10 or M7 and M12, tend to have similar performance for all seasons, suggesting the atmospheric model may be a primary source of precipitation biases.

What causes the seasonal dependence of the prediction of climatological seasonal mean precipitation? It is found

**Fig. 2** The pattern correlation coefficient (PCC) of the individual model ensemble and their multi-model ensemble prediction for annual mean and four seasons, respectively, over the globe



that the current coupled models better simulate spatial distribution of climatological SST in JJA and DJF than in MAM and SON. During MAM, large negative SST biases are found over the North Indian Ocean (IO) that is related to negative precipitation biases over the same region. On the other hand, positive (negative) SST biases are found over the Philippine Sea and equatorial western Pacific in SON season which is possibly related to enhanced (reduced) precipitation over the Philippine Sea (East Asia region) (not shown). The seasonal dependence of respective forecast skill is also related to the asymmetric distribution of seasonal precipitation between boreal and austral summer and between boreal and austral spring, which result from the differences in the land-sea distribution and topography between the two hemispheres. It suggests that the performance on the annual mean, to a large extent, represent the average skill of the seasonal mean precipitation, and the performance of seasonal migration of precipitation can be evaluated using AC modes which will be described in the next subsection.

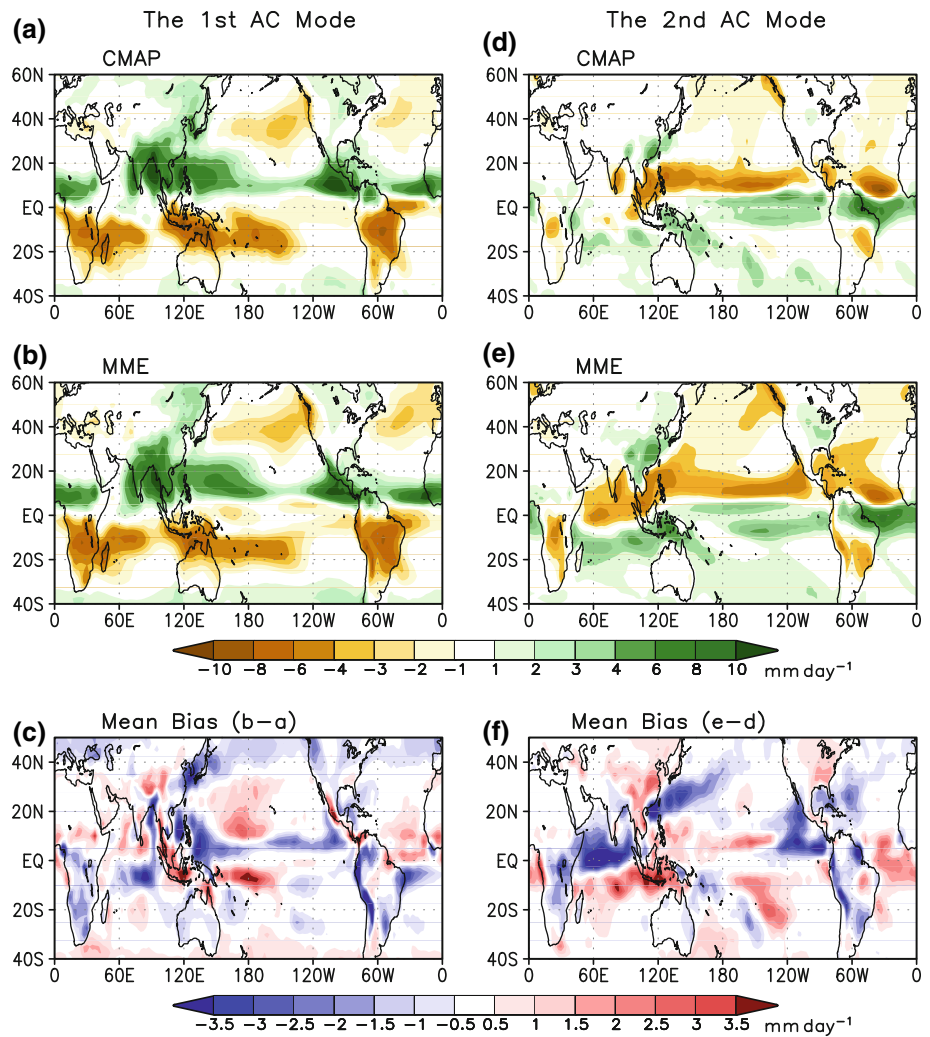
### 3.2 Annual cycle

Wang and Ding (2008) defined two annual cycle (AC) modes by EOF analysis of the climatological monthly mean precipitation. They have shown that the first two leading modes account for 71 and 13% of the total annual variance, respectively. The first mode represents a solstice global monsoon mode. Its spatial pattern can be represented extremely well by the difference between June–July–August–September (JJAS) and December–January–February–March (DJFM) mean precipitation. The second EOF mode has also an annual period with a maximum in April–May (AM) and minimum in October–November (ON). The second mode represents an equinox asymmetric mode and its spatial pattern can be very well represented by the difference between AM and ON. Hereafter, we will use the pattern of JJAS minus DJFM and AM minus ON to represent, respectively, the first and second AC modes.

In this study, the observed first two leading modes account for 68 and 15%, respectively, since we use different time period to obtain the leading modes from Wang and Ding (2008). It is shown in Fig. 3 that the first two AC modes of the one-month lead seasonal MME prediction are reasonably close to the observed counterparts. The major deficiencies with the predicted first mode are found over the Bay of Bengal, South China Sea (SCS), Philippine Sea, and East Asian monsoon front (Miyu-Baiu-Changma rain band). The bias implies that the MME predicted a weaker-than-observed Asian summer monsoon (Fig. 3c). We found that the large deficient rainfall bias over the SCS and Philippine Sea is related to the weak interannual variability over the same region. We speculate that the insufficient precipitation over those regions may in turn lead to reduced mean precipitation and its variability in East Asian summer monsoon region. This issue will be revisited in Sect. 6. Another large bias is found over the equatorial Eastern Pacific, tropical Atlantic and South America. The bias over the equatorial Eastern Pacific may be related to SST cold bias which most couple models exhibit. The MME prediction tends to have a stronger AC over the tropical Atlantic convergence zone and weaker South Africa and South American monsoon.

The second AC mode, or the spring-fall asymmetric mode, is captured reasonably well by the MME prediction (Fig. 3e) but with less fidelity than the first mode with due regard to their respective amplitudes. On the whole, the MME prediction exaggerates the spring-fall asymmetry compared to the observation, especially over the entire IO, Maritime Continent and East Asia. The strengthening of spring-fall asymmetry over the entire IO sector is likely linked to the following two major biases in spatial distribution of precipitation: (1) The predicted rainfall band shifts northward from 10°S in AM to Equator in ON, while the center of observed one does not change, persisting around Equator in both AM and ON although the ON precipitation is stronger than the AM one, and (2) the MME tends to predict zonally oriented rainfall band and has

**Fig. 3** The spatial pattern of differential precipitation between **a, b** June–September and December–March (JJAS–DJFM), and **d, e** between April–May and October–November (AM–ON) in observation and multi-model ensemble prediction. **c, f** Biases of the multi-model ensemble prediction against observation (CMAP) for each mode. The unit is mm/day



difficulty in capturing the observed distinct east–west asymmetry characterized by strong precipitation over Eastern IO and weak precipitation over the Western IO in AM (not shown).

The exaggerated spring–fall asymmetry over East Asia is mainly due to a positive bias of precipitation over the continental East Asia and a negative bias over the oceanic region in AM and a positive bias over the Philippine Sea in ON. The negative bias in the eastern Pacific ITCZ results from overestimating (underestimating) of ITCZ in ON (AM).

In the observation, there are several hypotheses trying to explain the asymmetry especially over the A–AM region which include: (1) a combination of asymmetric wind–terrain interaction and asymmetric low-level divergence induced by different land–ocean thermal inertia over A–AM region (Chang et al. 2005; Wang and Ding 2008), and (2) seasonally varying east–west SST gradients over the equatorial Pacific and the Indian Oceans (Webster et al. 1998). In the coupled models, the systematic bias in north–south SST gradient during April–May would play a role in strong spring–fall asymmetry over the entire IO and the

strong positive SST bias over the WNP in October–November would be one of the error sources for the strong asymmetry over the East Asian and WNP region (not shown). In particular, most of coupled models have cold bias over the North IO and weaker north–south SST gradients over the entire IO, possibly resulting in weakening of precipitation over the Bay of Bengal and Eastern IO in April and May.

The performance of the individual coupled model ensemble (ME) and their MME for simulating AC is evaluated objectively by using Pattern Correlation Coefficient (PCC) and normalized root mean square error (NRMSE) over the global tropics and subtropics (0°E–360°E, 40°S–40°N). The NRMSE is the RMSE normalized by the observed standard deviation that is calculated against area mean of the observed precipitation over the region. Figure 4 shows that the current coupled models can reproduce the observed first AC mode realistically but they have difficulty in simulating the second AC mode. They show a large spread in both PCC (0.55–0.8) and NRMSE (0.78–1.18) for the second AC mode. However, the MME has evidently a

reasonable degree of skill: the PCC for the first mode (second mode) is 0.94 (0.83) and the NRMSE is 0.33 (0.62), respectively. It is noted that the linear relationship between the two skill measures is weaker for the second mode (Fig. 4b) compared to the first mode (Fig. 4a). The weaker linear relationship possibly indicates that individual model's error is more independent from each other compared to that for annual mean and the first AC mode. It is also found that in terms of the two annual cycle modes, one cannot name a so-called best model or worst model in all measures. The M2 is the best model as far as the NRMSE is concerned, but not for PCC. The M8 is the worst model in terms of NRMSE but not the PCC. M13 is the best model in terms of PCC of the first two AC modes.

### 3.3 The predicted AC as a function of forecast lead time

For the sake of long-range forecast, it is important to know the model's behavior with respect to forecast lead time.

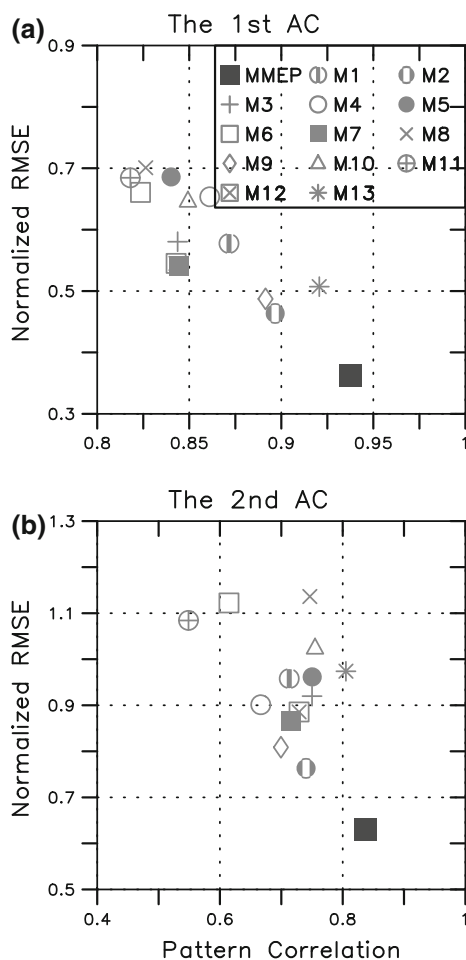


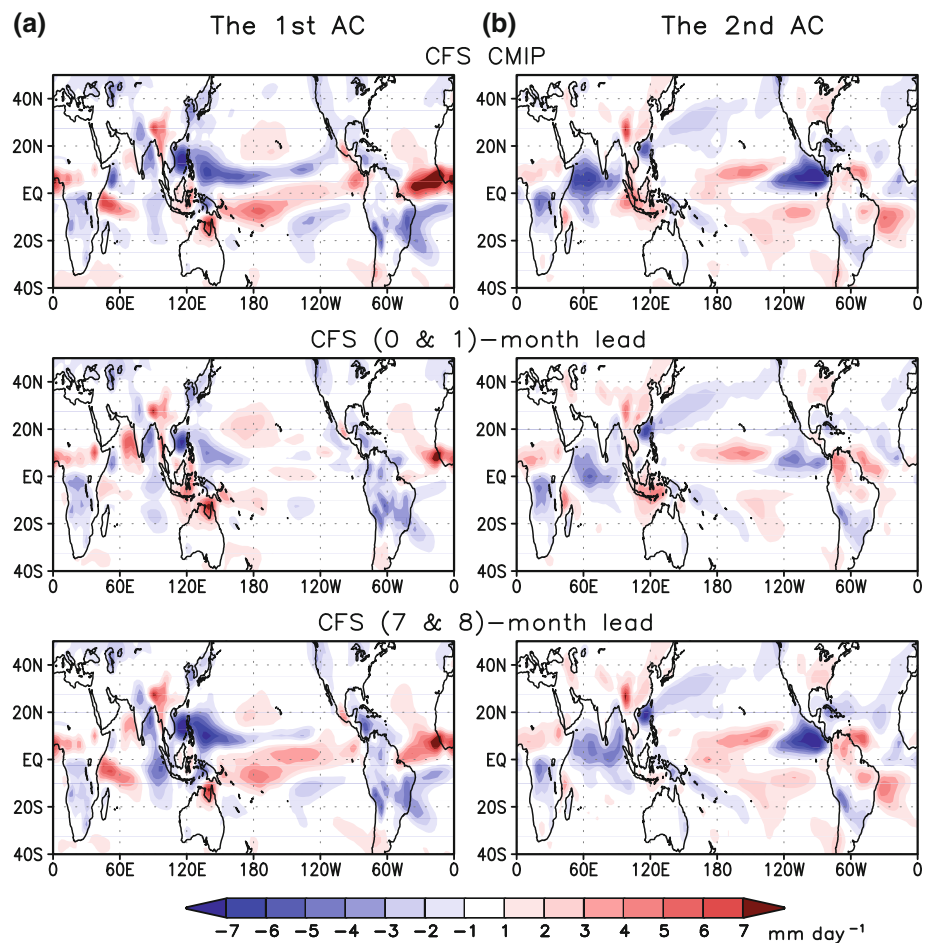
**Fig. 4** Forecast skill for **a** the first and **b** the second AC of precipitation in terms of PCC and NRMSE over the globe ( $0^{\circ}\text{E}$ – $360^{\circ}\text{E}$ ,  $40^{\circ}\text{S}$ – $40^{\circ}\text{N}$ ) in MME and individual ME predictions

The NCEP CFS data are best suited for this purpose, because the CFS prediction is issued 12 times a year with up to 9-month forecast lead time. Saha et al. (2006) described the characteristics of climate drift in CFS prediction with forecast lead time during DJF and JJA seasons. They indicated that the major biases exist in the tropics, no matter what season or what forecast lead, and the systematic biases get stronger as the lead time increases. Here, we assess the model's capability in prediction of the first and second AC modes as functions of forecast lead time in comparison with free coupled (CMIP) runs in order to identify the model's inherent systematic errors, and the impact of initial conditions. The four different realizations of CMIP runs with the same coupled model (CFS) were used for 30-year integrations. Thus, the total number of the integration years for the CMIP run is 120. The obtained climatology may reveal the intrinsic bias of the CFS model.

Comparison of the CFS 1-month lead forecast and CMIP shows that the initial condition of the coupled prediction tends to significantly reduce the model's intrinsic systematic errors in the CMIP runs, especially over the oceanic convergence regions in the north- and southwestern Pacific, south IO, and tropical Atlantic (Fig. 5). As the forecast lead time increases, the systematic biases of CFS forecast resemble more closely to those of the free coupled run. It is also noted that the initial condition of the coupled prediction cannot reduce the strong negative bias over the Bay of Bengal, Philippine Sea, South America, and East Asia, indicating that the reduction of precipitation over those regions is an inherent problem of CFS model.

Figure 6 shows the PCCs of the CFS predicted first and second AC modes as a function of forecast lead time. The PCCs were computed against the CMAP observation (square) and the CMIP run (circle), respectively. The computation domain covers the global tropics and subtropics. The results in Fig. 6 raise several interesting issues about the model's performance at various forecast lead time in relation to the properties of the coupled model itself. As the forecast lead time increases, the spatial pattern of the predicted AC modes tend to drift away from the observation (as indicated by the decreasing PCC with CMAP) while resembling closer to the coupled model's inherent AC modes (as indicated by the increasing PCC with the CMIP AC modes). It is also noted that the evolution of skill with forecast lead time is not a linear function. For the first mode, the CFS prediction skill keeps a high level up to 5-month lead and then decreases with forecast lead time. On the other hand, the forecast skill of the second mode decreases rapidly up to 3-month lead time and then keeps similar level of value afterward. It is also noted that the predicted AC modes are more closely related to the CMIP AC than the observed even at zero-month

**Fig. 5** The systematic bias of simulated **a** the first AC and **b** the second AC mode of precipitation using CFS CMIP simulation, CFS 0 and 1-month lead forecast and CFS 7 and 8 month lead forecast



lead, suggesting correction of the inherent bias in the mean state is critical for improving seasonal prediction even at short-lead forecast time. We also investigated the NRMSE skill and found that the characteristics of the skill as a function of forecast lead time are very similar to that of PCC skill presented here.

#### 4 Evaluation on global and regional monsoon climatology

In this section, we examine coupled model's capability in simulating the global monsoon rain domain and in capturing the seasonal march of regional monsoon precipitation over the Asian–Australian monsoon region.

##### 4.1 The global monsoon rain domain

Here we use the monsoon rain domain as one of the metrics to evaluate coupled model's capability in simulating seasonal distribution of precipitation. According to Wang and Ding (2006), the “monsoon rain domain” is defined as the regions in which the annual range of precipitation rate

exceeds 2 mm/day and the local summer monsoon precipitation exceeds 35% of annual rainfall. The annual range of precipitation is measured by the local summer-minus-winter precipitation, i.e. JJA-DJF for the northern hemisphere and DJF-JJA mean precipitation for the southern hemisphere.

Figure 7 shows the monsoon domain derived from CMAP climatology (blue contour) and the one-month lead seasonal MME prediction (red contour). The predictions realistically capture the major monsoon domains in South Asia, Indonesia–Australia, North and South Africa, and Central and South America. However, the MME prediction has difficulty in capturing the WNP tropical monsoon regions and the East Asian subtropical monsoon (Maiyu-Baiu) region. In the East Asian subtropical and WNP monsoon regions, the coupled models show a large discrepancy in terms of defining the monsoon (Fig. 7b). The model spread in these regions is depicted by the number of models which correctly capture monsoon seasonal cycle at each grid point. Gray color indicates that all 13 models capture monsoonal precipitation characteristics at the point. The deficiency arises from the fact that some models cannot predict correctly the seasonal distribution of

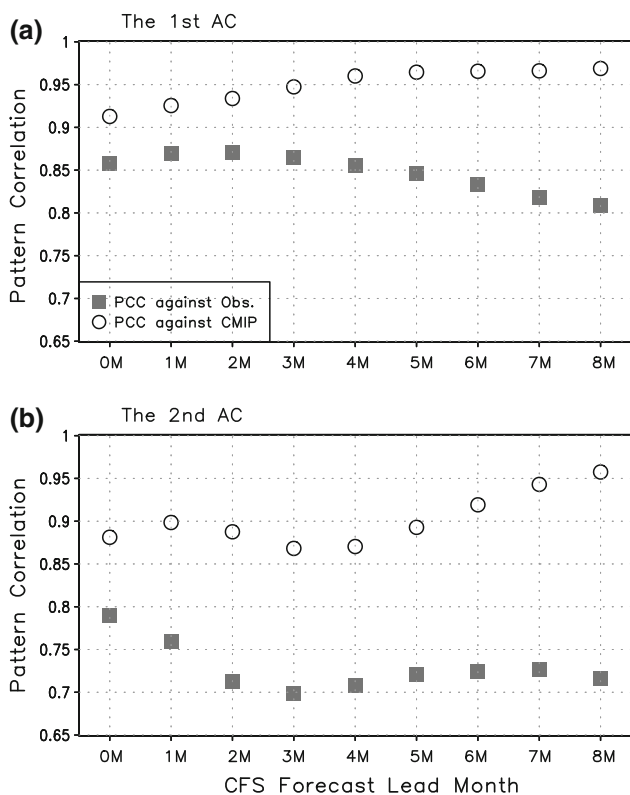


**Fig. 6** The PCC of **a** the first and **b** the second AC modes of CFS prediction as a function of forecast lead time against CMAP observation and against CMIP run over the globe

precipitation in the East Asian subtropics and WNP, nor in the southwest Indian Ocean monsoon regions. There is an urgent need to improve the major deficiency of the current coupled models in simulating WNP and EA monsoon system.

#### 4.2 Rainy season of regional monsoon systems

In this section, we examine how the seasonal march of regional monsoon precipitation was captured by the one-month lead seasonal coupled predictions. For this purpose, we used only seven coupled models in which the daily precipitation data are available for four seasons. For simplicity, we focus on area-averaged precipitation over four major sub-domains of the A-AM system: Indian Monsoon (IM, 5°N–30°N, 60°E–105°E), WNP Monsoon (WNPM, 5°N–20°N, 105°E–160°E), East Asian Monsoon (EAM, 20°N–45°N, 110°E–140°E), and Australian Monsoon (AusM, 20°S–5°S, 105°E–160°E) regions. The IM and WNPM include the precipitation over the Bay of Bengal and the Philippine Sea, respectively, where the largest amount of latent heat is released in association with the heaviest precipitation in the Asian summer monsoon.

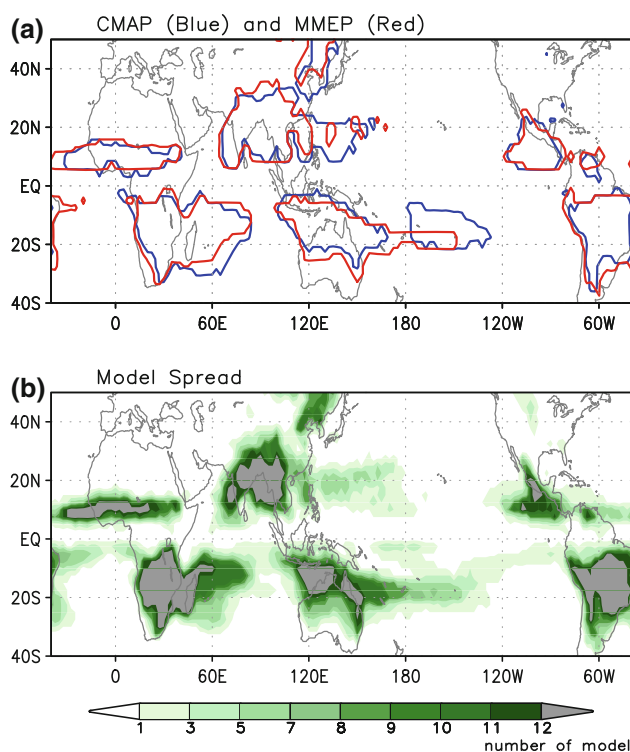


**Fig. 7** **a** The monsoon rain domain derived from observed precipitation (CMAP) and the one-month lead multi-model ensemble prediction. **b** The number of model which captures the monsoon domain at each grid point. The definition of monsoon domain is referred to the text

Figure 8 shows the predicted annual variation for the four precipitation indices in comparison with observations. Overall, the coupled models, especially their MME, can capture the seasonal march including the climatological onset and withdraw realistically over the all monsoon domains. Over the IM region, the MME and majority of the individual coupled models not only capture an abrupt increase of precipitation from mid-May to early June successfully, but also show similar magnitude of annual range with observation (Fig. 8a). However, stand-alone atmospheric models tend to overestimate summer rainfall over the IM region (as shown in Fig. 2a of Wang et al. 2004).

On the other hand, the coupled model MME prediction has considerable biases in both amplitude and phase over the WNP region (Fig. 8b), which are characterized by underestimation of summer rainfall (especially from mid July to late August) and overestimation of winter and spring rainfall in conjunction with much larger model spread compared to the IM counterpart. Nevertheless, the model spread from MME in the current coupled models is significantly less than that in the AGCM simulations (Fig. 2b of Wang et al. 2004). It is not clear though whether this improvement is due to improved atmospheric

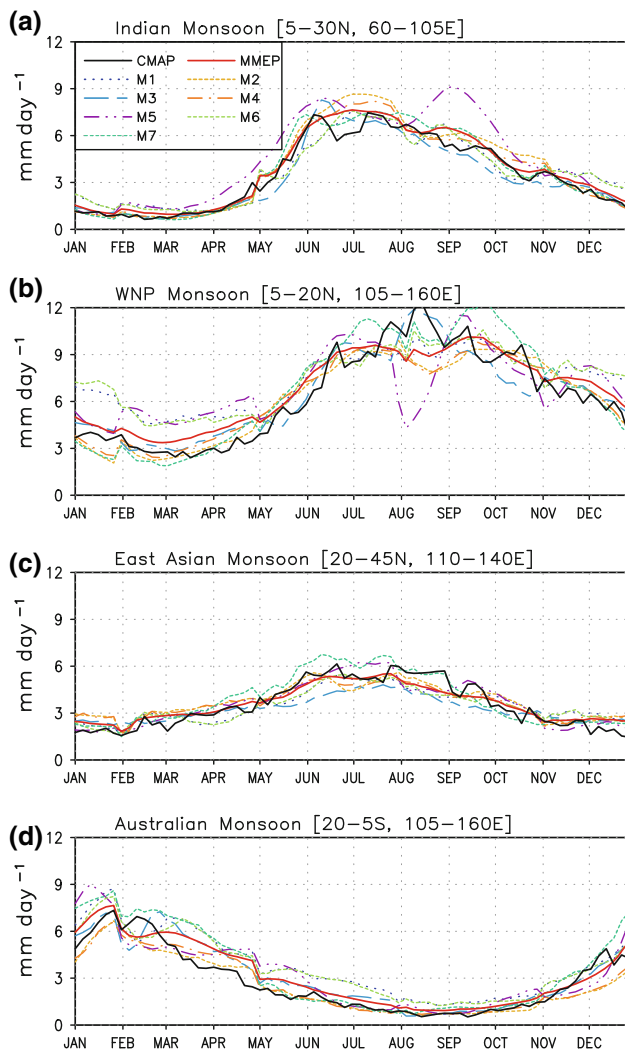


**Fig. 8** Time series of climatological pentad mean precipitation averaged over **a** Indian monsoon and **b** Western North Pacific, **c** East Asian monsoon, and **d** Australian monsoon regions obtained from CMAP, MME and individual ME predictions which participate in DEMETER projects

models or due to inclusion of the atmosphere–ocean coupling.

Over the EAM region, the annual variation of the MME prediction is in good agreement with the observed counterpart. However, most models tend to underestimate the second peak during late July to mid September, during which tropical cyclones account for a significant amount of precipitation in this region but the models are unable to resolve adequately the tropical cyclone rainfall (Kang et al. 1999; Wang and Linho 2002). The AC of the AusM precipitation is also well depicted by the MME and individual coupled predictions shown in Fig. 8d. However, the MME significantly overestimates the austral fall (March–May) rainfall, and the model spread from MME is very large during austral summer, reducing the signal-to-noise ratio.

## 5 Relationship between mean performance and climate prediction skill

In this section, we first raise possibility that the systematic model errors in mean field may affect interannual variability of the simulated precipitation anomaly and degrade its forecast skill, and then examine relationship between the skill in mean state and that for the seasonal precipitation anomalies in current coupled models and their MME. We also discuss how the SST mean performance is related with the forecast skill of seasonal SST anomalies and in turn with the skill of seasonal precipitation anomalies.

### 5.1 Mean versus interannual variability

Results in Fig. 7a and 8b indicate that the most striking deficiency of the one-month lead coupled prediction is underestimating the precipitation over the SCS and WNP regions, which is one of the most important atmospheric heat sources that drive atmospheric circulation. How does this mean bias link with the bias of seasonal anomalies over that region?

Figure 9 shows the climatological mean (June–July–August (JJA) precipitation and its corresponding variance for 21 years over the WNPM region obtained from CMAP and individual coupled model predictions, as well as the averaged value of individual model predictions. The majority of coupled models not only under-predict climatological mean precipitation but also the interannual variability of seasonal anomalies. Since the variance of each model was calculated using its ensemble mean, the reduced amplitude in variance is expected. However, the magnitudes of variances in most coupled models are less than half of the observed over the region. Over the IM region, on the other hand, the magnitudes of the simulated variability are comparable or slightly less than that of the observed one. It is also shown in Fig. 9 that the model which has larger climatological mean tends to have larger variance.

One possible reason for the weak variability is the deficiency of the model in simulating intraseasonal oscillation over the region (Waliser et al. 2003a, b). Previous studies have shown that there is a positive relationship between subseasonal and interannual variability over Asian monsoon region in AGCMs (Sperber et al. 2000, 2001; Goswami et al. 2006). Further study is needed to address the role of ISO on seasonal mean and its interannual variability in coupled models.

It is also seen from our results that the most coupled models produce very weak anomalies over the midlatitude, including the East-Asia summer monsoon region (not shown), resulting in a very low forecast skill there. Our further study is suggested that underestimation of

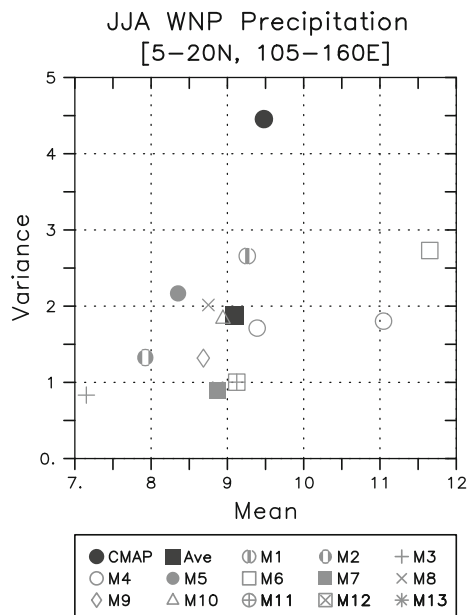


**Fig. 9** Scatter diagram of the climatological mean of JJA precipitation versus its variance for 21 years averaged over the WNP region obtained from CMAP, the individual coupled ME predictions and the averaged value of the individual prediction

precipitation amount and the interannual variability over the WNP region is a possible source of errors that compromises seasonal prediction skill over the EA and north Pacific region.

## 5.2 Relationship between the model climatology and seasonal forecast

As reviewed in the introduction, many previous studies have found that in the stand-alone atmospheric models forced by observed SST, a relationship between the fidelity of a model in simulating climatology (or seasonal migration) and the model's ability to simulate seasonal anomalies exists. Here, we evaluate the coupled model's capability in capturing annual modes and seasonal anomalies using 1-month lead seasonal predictions. Although the coupled models include air–sea interaction, they have the disadvantage in maintaining the long-term climate mean state.

The relationship between the prediction skill of the annual modes and that of seasonal anomalies is examined in a simple way. Figure 10a shows the scatter diagram of PCC for forecast annual mean versus forecast seasonal anomalies over the global tropics and subtropics (total of 84 seasons). To obtain averaged seasonal forecast skill, the anomaly PCCs have been first calculated over the global tropics and subtropics, every year for each season, respectively, after removing climatological mean at each grid points in observation and prediction, and then

their 21-year time mean and four seasonal mean have been taken. Figure 10b shows relationship between the performance in the AC and the performance in predicting all seasonal anomalies. To evaluate the AC prediction, we have combined the skills of the first and second AC modes by weighting their eigenvalues of EOF analysis as follows.

$$PCC_{AC} = \lambda_{AC1}PCC_{AC1} + \lambda_{AC2}PCC_{AC2},$$

Where  $\lambda_{AC1}$  and  $\lambda_{AC2}$  are the eigenvalues of the first and second AC modes, respectively.  $PCC_{AC1}$  and  $PCC_{AC2}$  are the pattern correlation coefficients of the predicted first and second AC eigenvectors, respectively, against observation. For the MME prediction, the first AC mode accounts for 68% of total variance and the second AC mode accounts for 17%, which is in a reasonably good agreement with observation (68 and 15%, respectively) although the most of coupled models underestimate the percentage variance of the first mode and slightly overestimate that of the second mode.

Results shown in Figs. 10a, b reveal several interesting points. First, the MME prediction has much better skill than individual ME prediction for both mean state and seasonal anomalies. In particular, the improvement of prediction through MME approach is prominent for the second AC mode in which individual model's error is more independent each other than in the annual mean and the first AC mode (not shown).

Second, the seasonal prediction skills are positively correlated with their performances on both the annual mean and AC in the coupled retrospective forecasts. The correlation coefficient between seasonal prediction skill and annual mean (AC) is 0.31 (0.55). However, for some models, such as M6, M8, and M10, they have lower skills in both the annual mean and AC, but have higher skills in seasonal prediction. It is found that those models tend to highly exaggerate the mean precipitation over Maritime Continents and high elevated terrains than other models, compromising pattern correlation skill of the mean field. Terrain-related precipitation, however, tend to have weak interannual variability in both observation and prediction. Thus, anomaly errors in those coupled models over the mountain regions are relatively small in spite of large errors in their climatological simulation.

Third, the 1-month lead seasonal prediction of precipitation using the 13 coupled models' MME has a similar level of skill with both ERA-40 and NCEP-R2 precipitation in terms of not only the mean state (climatology) but also the seasonal anomaly prediction. Although the comparison between the MME and a single realization of reanalysis precipitation may not be fair, the improvement of coupled models is promising. In addition, the results here support and confirm the results of Wang et al. (2008). They showed that the one-month lead coupled models'

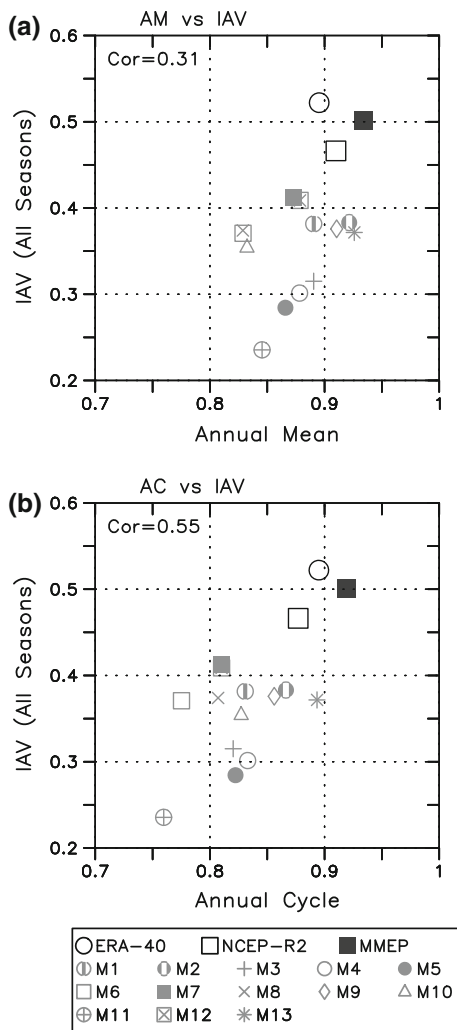


**Fig. 10** **a** Scatter diagram between the pattern correlation skill of annual mean and that of seasonal anomalies for all seasons over the globe derived from MME and individual ME predictions. **b** Same as (a) except for the first two annual cycle modes instead of annual mean. For comparison, the skills of reanalysis precipitation from ERA-40 and NCEP-R2 are shown

MME seasonal prediction captures the first two dominant modes of interannual variability of A-AM precipitation better than the two reanalysis data, although it has difficulty in capturing variability associated with the higher modes, which are presumably less predictable. If we consider all modes of interannual variability of precipitation over the global tropics and subtropics, the anomaly PCC skill for seasonal precipitation is 0.5 for all season using the state-of-the-art one-month lead coupled MME prediction, which is comparable to those of two reanalysis skills. Wang et al. (2008) have analyzed the possible reasons and proposed that the future reanalysis should be carried out with coupled atmosphere and ocean models.

We further found that the linear relationship between simulation of climatology and seasonal anomaly prediction

depends on season (Fig. 11). The relationship is the most strongest in JJA with a correlation coefficient of 0.77 and the lowest in DJF with a correlation coefficient of 0.22. The correlation coefficient is 0.66 in MAM and 0.58 in SON. Figure 11 reveals that the improvement of model climatology in JJA is an important factor for skillful prediction of the waxing and waning of the Asian summer monsoon precipitation. On the contrary, the systematic biases on mean state have a less impact on the performance in predicting interannual variability of precipitation in DJF.

### 5.3 Impact of SST mean performance

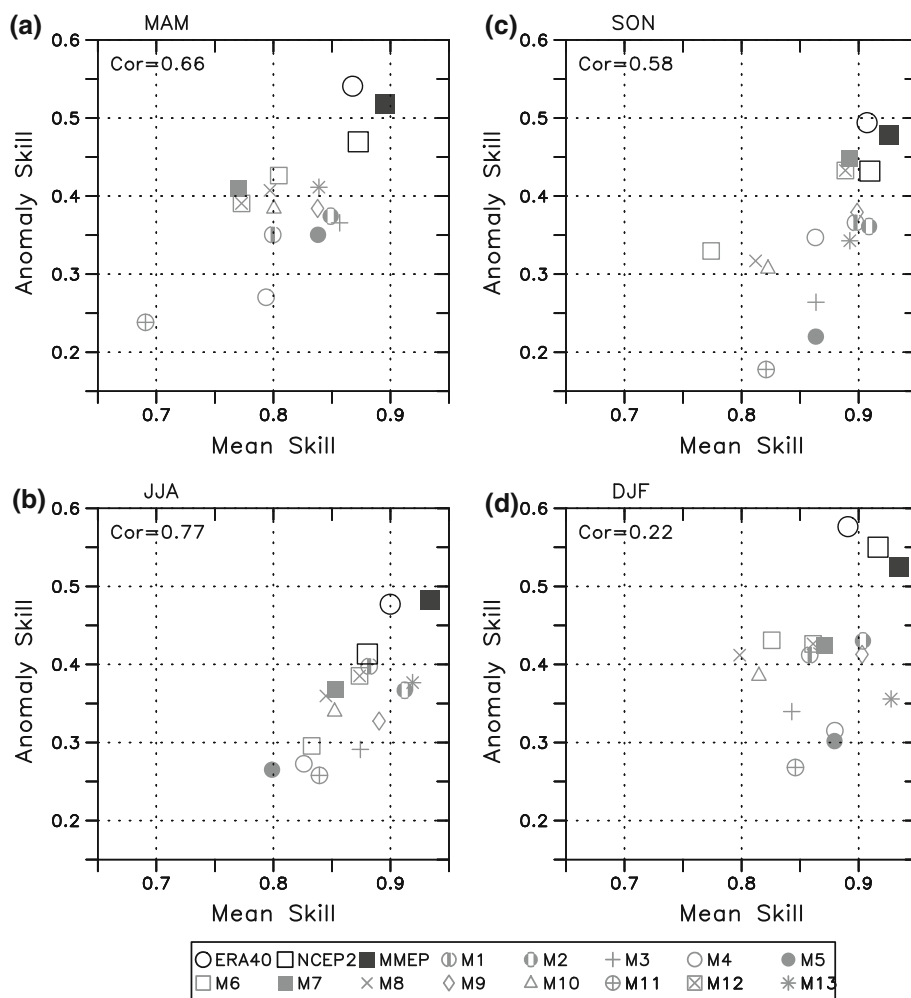
Wang et al. (2007, 2008, 2009) demonstrated that ENSO is a dominant predictability source for the global tropical precipitation in the current coupled models. Analysis reveals that the PCC skill for seasonal SST anomaly is strongly linked to that for seasonal precipitation anomaly over the global Tropics between 20°S and 20°N among couple models with a correlation coefficient of 0.81, 0.86, 0.83, and 0.82 in MAM, JJA, SON, and DJF, respectively. Since previous studies have suggested that the coupled models' ability to simulate the SST mean state plays an important role on simulating realistic interannual variability (Schopf and Suarez 1988; Battisti and Hirst 1989; Li and Hogan 1999; Vintzileos et al. 1999; Jin et al. 2008), we further examine the relationship between the SST mean performance and SST seasonal prediction over the global Tropics between 20°S and 20°N.

Figure 12 indicates that the models' SST mean performance is positively correlated with the models' ability to predict seasonal SST anomalies. The relationship is particularly strong in SON (a correlation coefficient of 0.84) and JJA (0.77). The MME skill is much better than that of persistent SST forecast for both mean performance and seasonal SST prediction. Jin et al. (2008) and our further study indicate that the SST mean bias is closely related to the errors in amplitude, phase, and maximum location of ENSO variation which may result in errors in ENSO-monsoon relationship and then in degrading monsoon prediction.

## 6 Conclusion

Knowledge of the model performance in simulation and forecast of seasonal mean states is necessary for assessing and understanding of the model's capability in predicting seasonal anomalies, especially when the variable of interest strongly depends on seasonal variation such as precipitation. In order to gauge model's performance on climatological precipitation, we adopted a simple objective metrics which consists of four major components: the annual mean,

**Fig. 11** Scatter diagram between the pattern correlation skill of seasonal mean climatology and that of seasonal anomalies for **a** MAM, **b** JJA, **c** SON, and **d** DJF, respectively, over the globe derived from MME and individual ME predictions. For comparison, the skills of reanalysis precipitation from ERA-40 and NCEP-R2 are shown



the two leading modes of the AC, and the monsoon rain domain. To evaluate the current status of model's capability in capturing mean states and seasonal anomalies, 1-month lead seasonal retrospective forecasts of 13 coupled atmosphere–ocean models have been examined for 21 years (1981–2001) obtained from APCC/CliPAS and DEMETER projects.

The state-of-the-art coupled models can reproduce realistically the observed features of long-term annual mean precipitation with a similar level of skill as that of ERA-40 and NCEP-R2 reanalysis (Fig. 1). However, these models have common biases over the oceanic convergence zones where SST bias exists and the regions where the wind–terrain interaction is prominent. The 1-month lead seasonal MME prediction also captures well the first two AC modes (Fig. 3). However, the models tend to underestimate the annual ranges over the Bay of Bengal, South China Sea (SCS), Philippine Sea, and Maiyu-Baiu-Changma frontal regions, implying that the models underpredict Asian summer monsoon strength to a certain extent. On the other hand, the models tend to exaggerate the

spring–fall asymmetry over the entire Indian Ocean, East Asia and SCS and Philippine Sea regions.

The initial condition of the coupled model prediction plays an important role in reducing the systematic biases over the oceanic convergence regions. As the forecast lead time increases, the systematic biases of CFS prediction tend progressively similar to those of the CFS free coupled run (Fig. 5). It is also noted that the predicted AC modes are more closely related to the CMIP AC modes than the observed event at zero-month lead. This result suggests that correction of the inherent bias in the mean state is critical for improving the seasonal prediction.

The MME prediction replicates the monsoon precipitation domain very well except in the East Asian subtropical monsoon and the tropical western North Pacific (WNP) summer monsoon regions (Fig. 7). The coupled models can also capture the gross features of the seasonal march of the rainy season including onset and withdraw realistically over four sub-domains of the Asian–Australian monsoon system, i.e. the Indian monsoon, East Asian monsoon, western North Pacific monsoon, and Australian monsoon

**Fig. 12** Same as Fig. 11 except for the global Tropical SST between 20°S and 20°N. For comparison, the skill of persistent SST forecast is shown

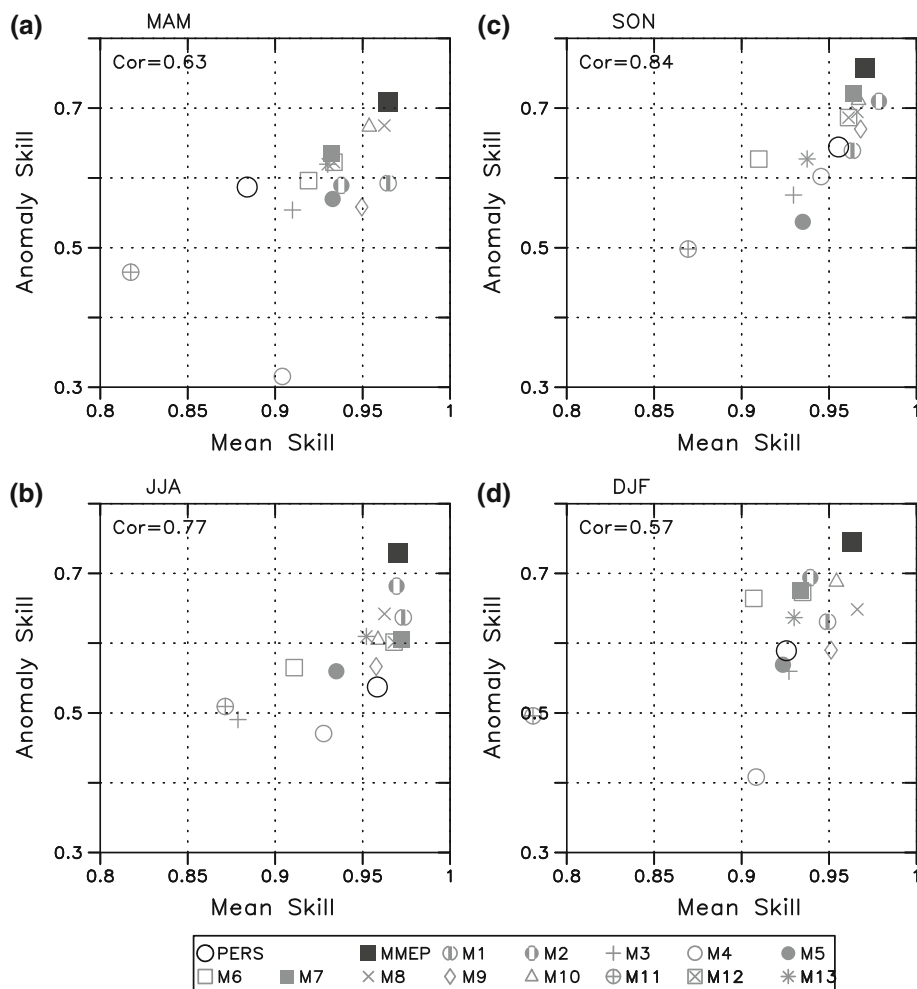


(Fig. 8). Again, the MME prediction has considerable biases in both the amplitude and phase over the WNP region (Figs. 8, 9).

The seasonal prediction skills for precipitation are positively correlated with their performances on both the annual mean and annual cycle of precipitation in the coupled climate models (Fig. 10). The MME prediction has considerably better skill than individual model prediction in terms of the given metrics. Note that the 1-month lead seasonal prediction made by the 13-model ensemble has skills that are much higher than those in individual model ensemble predictions and approached to those in the ERA-40 and NCEP-2 reanalysis in terms of both the precipitation climatology and seasonal anomalies.

The seasonal prediction skill for the tropical SST anomalies, which are the major predictability source of monsoon precipitation in the current coupled models, is closely link to the models' ability in simulating the SST mean state. This study indicates that correction of the inherent bias in the mean state of precipitation and SST is

critical for improving the long-lead seasonal prediction of precipitation.

**Acknowledgments** This research was supported by APEC Climate Center (APCC) as a part of APCC International research project and the Korean meteorological Administration Research and Development Program under Grant CATER 2009-1146. Lee and Wang acknowledge support from IPRC, which is in part supported by JAMSTEC, NOAA (grant No. NNX07AG53G), and NOAA (grant No. NA09OAR4320075). This is the IPRC publication 703 and SOEST publication 7947.

**References**

Annamalai H, Liu P (2005) Response of the Asian summer monsoon to changes in El Nino properties. *Q J R Meteorol Soc* 131:805–831  
 Annamalai H, Slingo JM, Sperber KR, Hodges K (1999) The mean evolution and variability of the Asian summer monsoon: comparison of ECMWF and NCEP-NCAR reanalyses. *Mon Weather Rev* 127:1157–1186  
 Annamalai H, Hamilton K, Sperber KR (2007) The south Asian summer monsoon and its relationship with ENSO in the IPCC AR4 simulation. *J Clim* 20:1071–1092

- Battisti DS, Hirst AC (1989) Interannual variability in the tropical atmosphere–ocean system: influence of the basic state, ocean geometry, and non-linearity. *J Atmos Sci* 46:1687–1712
- Chang CP, Wang Z, McBride J, Liu CH (2005) AC of Southeast Asia–Maritime Continent rainfall and the asymmetric monsoon transition. *J Clim* 18:287–301
- Delecluse P, Madec G (1999) Ocean modeling and the role of the ocean in the climate system. In: Holland WR, Joussaume S, David F (eds) *Modeling the Earth's climate and its variability*, Les Houches 1997, Elsevier Science, Amsterdam
- Delworth TL et al (2006) GFDL's CM2 global coupled climate models—Part I: formulation and simulation characteristics. *J Clim* 19:643–674
- Deque M (2001) Seasonal predictability of tropical rainfall: probabilistic formulation and validation. *Tellus* 53A:500–512
- Fennessy MJ, Kinter JL III, Kirtman B et al (1994) The simulated Indian monsoon: a GCM sensitivity study. *J Clim* 7:33–43
- Fu X, Wang B (2004) The boreal-summer intraseasonal oscillations simulated in a hybrid coupled atmosphere-ocean model. *Mon Weather Rev* 132:2628–2649
- Gadgil S, Sajani S (1998) Monsoon precipitation in the AMIP runs. *Clim Dyn* 14:659–689
- Goswami BN, Wu G, Yasunari T (2006) The AC, intraseasonal oscillations, and roadblock to seasonal predictability of the Asian summer monsoon. *J Clim* 19:5078–5099
- Gregory D, Morcrette JJ, Jakob C, Beljaars ACM, Stockdale T (2000) Revision of convection, radiation and cloud schemes in the ECMWF Integrated Forecasting System. *Q J R Meteorol Soc* 126:1685–1710
- Jin EK, Kinter JL, Wang B, Park CK, Kang IS et al (2008) Current status of ENSO prediction skill in coupled ocean–atmosphere models. *Clim Dyn* 31:647–664
- Kanamitsu M, Ebisuzaki W, Woollen J, Yang S-K, Hnilo JJ, Fiorino M, Potter GL (2002) NCEP-DOE AMIP-II Reanalysis (R-2). *Bull Am Meteorol Soc* 83:1631–1643
- Kang IS, Ho CH, Lim YK, Lau KM (1999) Principal modes of climatological, seasonal, and intraseasonal variations of the Asian summer monsoon. *Mon Weather Rev* 127:322–340
- Kang IS, Jin K, Wang B, Lau KM, Shukla J et al (2002) Intercomparison of the climatological variations of Asian summer monsoon precipitation simulated by 10 GCMs. *Clim Dyn* 19:383–395
- Kitoh A, Arakawa O (1999) On overestimation of tropical precipitation by an atmospheric GCM with prescribed SST. *Geophys Res Lett* 26:2965–2968
- Kug J-S, Kang I-S, Choi D-H (2008) Seasonal climate predictability with tier-one and tier-two prediction system. *Clim Dyn* 31:403–416. doi:10.1007/s00382-007-0264-7
- Kumar KK, Hoerling M, Rajagopalan B (2005) Advancing Indian monsoon rainfall predictions. *Geophys Res Lett* 32:L08704
- Lau NC, Nath MJ (2000) Impact of ENSO on the variability of the Asian–Australian monsoon as simulated in GCM experiments. *J Clim* 13:4287–4309
- Li T, Hogan TF (1999) The role of the annual-mean climate on seasonal and interannual variability of the Tropical Pacific in a coupled GCM. *J Clim* 12:780–792
- Luo J-J, Masson S, Behera S, Shingu S, Yamagata T (2005) Seasonal climate predictability in a coupled OAGCM using a different approach for ensemble forecasts. *J Clim* 18:4474–4497
- Madec G, Delecluse P, Imbrad M, Levy C (1997) OPA release 8, Ocean general circulation model reference manual. LODYC Internal Report, Paris
- Madec G, Delecluse P, Imbrad M, Levy C (1998) OPA version 8.1, Ocean general circulation model reference manual. LODYC Technical Report No. 11, Paris
- Marsland SJ, Haak H, Jungclaus J-H, Latif M, Roske F (2003) The Max-Planck-Institute global ocean/sea ice model with orthogonal curvilinear coordinates. *Ocean Model* 5:91–127
- Mechoso CR, Robertson AW, Barth N, Davey MK, Delecluse P, Gent PR et al (1995) The seasonal cycle over the tropical Pacific in coupled atmosphere-ocean general circulation models. *Mon Weather Rev* 123:2825–2838
- Meehl GA, Arblaster JM, Loschnigg J (2003) Coupled ocean–atmosphere dynamical processes in the tropical Indian and Pacific Oceans and the TBO. *J Clim* 16:2138–2158
- Nanjundiah RS, Vidyumala V, Srinivasan J (2005) On the difference in the seasonal cycle of rainfall over India in the community climate system model (CCSM2) and community atmospheric model (CAM2). *Geophys Res Lett* 32:L20720. doi:10.1029/2005GL024278
- Palmer TN, Alessandri A, Andersen U, Cantelaube P, Davey M et al (2004) Development of a European multi-model ensemble system for seasonal to interannual prediction (DEMETER). *Bull Am Meteorol Soc* 85:853–872
- Roeckner E, Arpe K, Bengtsson L, Christoph M, Claussen M, Dumenil L, Esch M, Giorgetta M, Schlese U, Schulzweida U (1996) The atmospheric general circulation model ECHAM4: model description and simulation of present-day climate. Max Planck Institut für Meteorologie, Report No. 218, Hamburg, Germany
- Saha S, Nadiga S, Thiaw C, Wang J et al (2006) The NCEP climate forecast system. *J Clim* 19:3483–3517
- Schopf PS, Suarez MJ (1988) Vacillations in a coupled ocean–atmosphere model. *J Atmos Sci* 45:549–566
- Smith TM, Reynolds RW (2004) Improved extended reconstruction of SST (1854–1997). *J Clim* 17:2466–2477
- Sperber KR, Palmer TN (1996) Interannual tropical rainfall variability in general circulation model simulations associated with the atmospheric model intercomparison project. *J Clim* 9:2727–2750
- Sperber KR, Slingo JM, Annamalai H (2000) Predictability and the relationship between subseasonal and interannual variability during the Asian summer monsoon. *Q J R Meteorol Soc* 126:2545–2574
- Sperber KR et al (2001) Dynamical seasonal predictability of the Asian summer monsoon. *Mon Weather Rev* 129:2226–2248
- Turner AG, Inness PM, Slingo JM (2005) The role of the basic state in the ENSO-monsoon relationship and implications for predictability. *Q J R Meteorol Soc* 131:781–804
- Uppala SM, Kållberg PW, Simmons AJ, Andrae U, da Costa Bechtold V et al (2005) The ERA-40 re-analysis. *Q J R Meteorol Soc* 131:2961–3012
- Vintzileos A, Delecluse P, Sadourny R (1999) On the mechanisms in a tropical ocean–global atmosphere coupled general circulation model. Part II: interannual variability and its relation to the seasonal cycle. *Clim Dyn* 15:63–80
- Waliser DE, Jin K, Kang IS et al (2003a) AGCM simulations of intraseasonal variability associated with the Asian summer monsoon. *Clim Dyn* 21:423–446
- Waliser DE, Stern W, Schubert S, Lau KM (2003b) Dynamic predictability of intraseasonal variability associated with the Asian summer monsoon. *Q J R Meteorol Soc* 129:2897–2925
- Wang B, Ding Q (2006) Changes in global monsoon precipitation over the past 56 years. *Geophys Res Lett* 33:L06711. doi:10.1029/2005GL025347
- Wang B, Ding Q (2008) The global monsoon: major modes of annual variation in tropical precipitation and circulation. *Dyn Atmos Ocean* 44:165–183
- Wang B, Lin Ho (2002) Rainy season of the Asian–Pacific summer monsoon. *J Clim* 15:386–398

- Wang B, Kang I-S, Lee J-Y (2004) Ensemble simulations of Asian–Australian monsoon variability by 11 AGCMs. *J Clim* 17:803–818
- Wang B, Ding QH, Fu XH, Kang I-S, Jin K, Shukla J, Doblas-Reyes F (2005a) Fundamental challenge in simulation and prediction of summer monsoon rainfall. *Geophys Res Lett* 32:L15711
- Wang W, Saha S, Pan HL, Nadiga S, White G (2005b) Simulation of ENSO in the new NCEP coupled forecast system model. *Mon Weather Rev* 133:1574–1593
- Wang B, Lee JY, Kang IS, Shukla J, Hameed SN, Park CK (2007) Coupled predictability of seasonal tropical precipitation. *CLI-VAR Exch* 12:17–18
- Wang B, Lee JY, Kang IS, Shukla J, Park CK et al (2008) How accurately do coupled climate models predict the Asian–Australian monsoon interannual variability? *Clim Dyn* 30:605–619. doi:[10.1007/s00382-007-0310-5](https://doi.org/10.1007/s00382-007-0310-5)
- Wang B, Lee JY, Kang IS, Shukla J, Park CK et al (2009) Assessment of the APCC/ClipAS 14-model ensemble retrospective seasonal prediction (1980–2004). *Clim Dyn* 33:93–117
- Webster PJ (2006) The coupled monsoon system. In: Wang Bin (ed) *The Asian Monsoon*, Springer
- Webster PJ, Magana VO, Palmer TN, Shukla J, Tomas RA, Yanai M, Yasunari T (1998) Monsoons: processes, predictability, and the prospects for prediction. *Geophys Res Lett* 103:14451–14510
- Wolff JE, Maier-Reimer E, Legutke S (1997) The Hamburg Ocean primitive equation model. In: Deutsches Klimarechenzentrum Tech. Rep. 13, Hamburg, Germany
- Wu R, Kirtman B (2005) Roles of Indian and Pacific Ocean air–sea coupling in tropical atmospheric variability. *Clim Dyn* 25:155–170
- Xie P, Arkin PA (1997) Global precipitation: A 17-year monthly analysis based on gauge observations, satellite estimates, and numerical model outputs. *Bull Am Meteorol Soc* 78:2539–2558
- Zhong A, Hendon HH, Alves O (2005) Indian Ocean variability and its association with ENSO in a global coupled model. *J Clim* 18:3634–3649